Angewandte Chemie International Edition

CO₂ Conversion

International Edition: DOI: 10.1002/anie.201505730
German Edition: DOI: 10.1002/ange.201505730

Electrocatalytic Production of C3-C4 Compounds by Conversion of CO_2 on a Chloride-Induced Bi-Phasic Cu_2O-Cu Catalyst

*Seunghwa Lee, Dahee Kim, and Jaeyoung Lee**

Abstract: *Electrocatalytic conversion of carbon dioxide (CO_2) has recently received considerable attention as one of the most feasible CO_2 utilization techniques. In particular, copper and copper-derived catalysts have exhibited the ability to produce a number of organic molecules from CO_2. Herein, we report a chloride (Cl)-induced bi-phasic cuprous oxide (Cu_2O) and metallic copper (Cu) electrode (Cu_2O_{Cl}) as an efficient catalyst for the formation of high-carbon organic molecules by CO_2 conversion, and identify the origin of electroselectivity toward the formation of high-carbon organic compounds. The Cu_2O_{Cl} electrocatalyst results in the preferential formation of multi-carbon fuels, including n-propanol and n-butane C3–C4 compounds. We propose that the remarkable electrocatalytic conversion behavior is due to the favorable affinity between the reaction intermediates and the catalytic surface.*

Control of greenhouse gas emissions, typically carbon dioxide (CO_2), is of great importance to humankind.[1] As well as the environmental issues, developing alternative energy sources to fossil fuels is another important global challenge. To achieve these goals, electrocatalytic conversion of CO_2 into fuels has been explored as a possible technical solutions for mitigating the effects of rising concentrations of atmospheric CO_2, and for the conversion of CO_2 back into a usable energy source.[2–4] For the last two decades, a variety of metals (such as Ag, Au, Cu, Pb, and Sn) have been intensively studied as catalysts for CO_2 conversion in an electrolytic process.[2,5] Among these, Cu is unique in its capability to transform CO_2 into various organic compounds, such as methane (CH_4), ethylene (C_2H_4), and alcohols.[6] Although there are several methods available to speed up the CO_2 conversion reactions, there is still a strong need for improvements in the design and operation of efficient catalysts, and the understanding of the conversion reaction on the catalytic surface.

Notably, several recent reports have suggested using metal oxide catalysts, and there is an ongoing debate whether the oxide layer contributes to catalysis, or whether it only acts as a promoter of the well-structured metal catalysts.[7–9] Very recently, we demonstrated that an electrodeposited Cu_2O catalyst can enhance the selectivity for the formation of C_2H_4 over CH_4.[9] Contrary to several previous reports,[2,7] using surface analysis and depth profiling of the oxygen concentration in the electrode, we observed a residual oxide layer in the surface region on the bulk Cu_2O-derived Cu structure. Therefore, both the oxide-derived metallic layer and the surface oxide should be considered as key reaction sites in the selective CO_2 catalysis toward multi-carbon fuels.

Herein, we demonstrate the efficient conversion of CO_2 into multi-carbon fuels, particularly the C2, C3, and even C4 species chemicals, on an in situ formed Cl-induced bi-phasic Cu_2O–Cu (Cu_2O_{Cl}). Because of the chemoaffinity between chloride (Cl^-) and Cu, a uniquely shaped phase is formed by the application of a cathodic potential in the Cl-containing CO_2 electrolytic system[10] that is different from that formed when using a carbonate-containing CO_2 electrolytic system, the so-called oxygen-evacuated Cu_2O (Cu_2O_{OE}) observed in our previous study.[9] The use of a potassium chloride (KCl) electrolyte for the CO_2 conversion on the Cu_2O electrode leads to a higher suppression of the undesired hydrogen (H_2) production and the improved preservation of the Cu_2O phase than in potassium bicarbonate ($KHCO_3$).[10,11] Finally, we explore how the synergistic effects between the chloride modification and the Cu_2O structure improve the electrocatalysis by considering the residence time of the reaction intermediates to increase the length of the carbon chains of the fuels.

A transmission electron microscope (TEM) with energy dispersive spectroscopy (EDS) mapping technique was used to observe the Cu_2O experiencing the shape transformation and the slight increase in particle sizes compared with bare Cu_2O (Supporting Information, Figure S1).[9] The high-resolution TEM image (Figure 1) shows the lattice fringe spacings of 2.45 Å, 2.13 Å, and 2.08 Å according to the (111) and (200) facet directions of Cu_2O, as well as the Cu (111) facet direction, respectively.[12] Cu_2O_{Cl} nanoparticles appear to be transformed into a crystallographic cuboctahedral shape. In earlier reports, this transformation was explained by the effects of additives such as halogen anions leading to aggregation and electrocrystallization that enhance the Cu_2O stability.[10b,c] Further analysis of ex situ X-ray diffraction (XRD) and field emission scanning electron microscope (FE-SEM) EDS mapping data (Supporting Information, Figures S2, S3) confirmed that more Cu remained in the oxidized phase on the Cu_2O_{Cl} than on Cu_2O_{OE}.

To examine the Cu_2O_{Cl} catalytic activity and selectivity for CO_2 conversion, linear sweep voltammograms (LSVs) were obtained at a cathodic sweeping rate of $20\ mV\,s^{-1}$ in both N_2-

---

[*] S. Lee, D. Kim, Prof. Dr. J. Lee
School of Environmental Science and Engineering
Gwangju Institute of Science and Technology (GIST)
Gwangju 500-712 (South Korea)
E-mail: jaeyoung@gist.ac.kr

Prof. Dr. J. Lee
Ertl Center for Electrochemistry and Catalysis, RISE
Gwangju Institute of Science and Technology (GIST)
Gwangju 500-712 (South Korea)

Supporting information for this article, including experimental details, is available on the WWW under http://dx.doi.org/10.1002/anie.201505730.

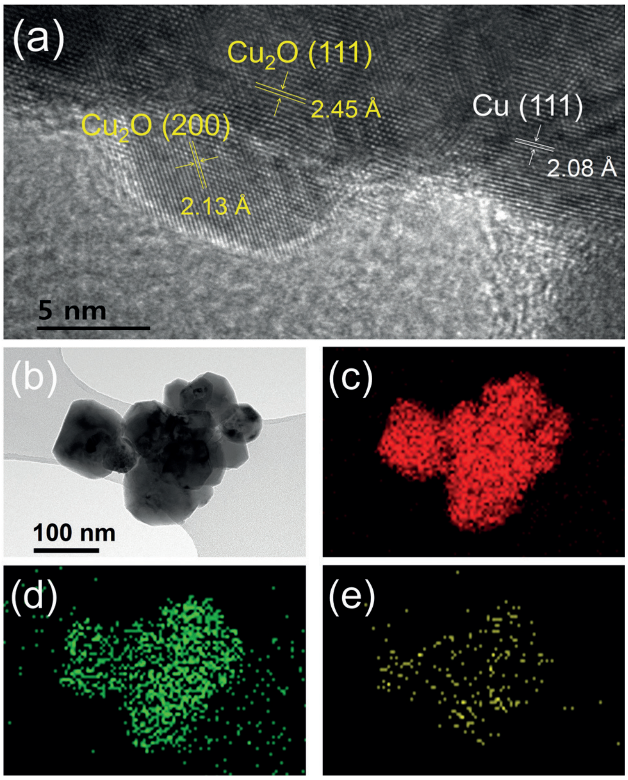

Figure 1. TEM images and EDS mapping results for the in situ transformed bi-phasic Cu_2O and Cu electrode (Cu_2O_{Cl}) by applied cathodic potential for 10 min in 0.1 M KCl. a) High-resolution and b) low-resolution TEM images of the Cu_2O_{Cl} and EDS mapping analysis identifying c) Cu, d) O, and e) Cl.

saturated and CO_2-saturated KCl solution. The CO_2-saturated solution exhibits a higher current value for the entire potential range because of the activation of CO_2 conversion and the inhibition of proton adsorption on the chloride ion-modified Cu_2O–Cu surface (Supporting Information, Figure S4).[11]

The potential dependence of the product distribution was evaluated between −0.6 V and −1.8 V (vs. RHE) in 0.1 M KCl (Figure 2a; Supporting Information, Figure S5). A number of organic compounds up to C4 species were generated (Supporting Information, Table S1 and Figure S6), and remarkably, *n*-propanol (C_3H_7OH) was obtained with an impressive Faradaic efficiency of 8.7% that is approximately 10-times higher than the value obtained in a previous study.[13] More interestingly, *n*-butane (C_4H_{10}) composed of four-carbon chains could be clearly detected. Production of C2 species such as C_2H_4 and C_2H_5OH with a total Faradaic efficiency of 55% was also observed. An early study by Jaramillo and coworkers found a total of 16 different CO_2 conversion products using Cu, but products with chains longer than three carbons were only detected, without obtaining a significant Faradaic efficiency.[13] Centi et al. demonstrated that CO_2 can be converted to long carbon chain hydrocarbons using Pt nanoparticles on a carbon-based material.[14] Nevertheless, this study represents the first report of direct electrochemical production of various C3–C4 products from CO_2 with Faradaic efficiencies over 10%.

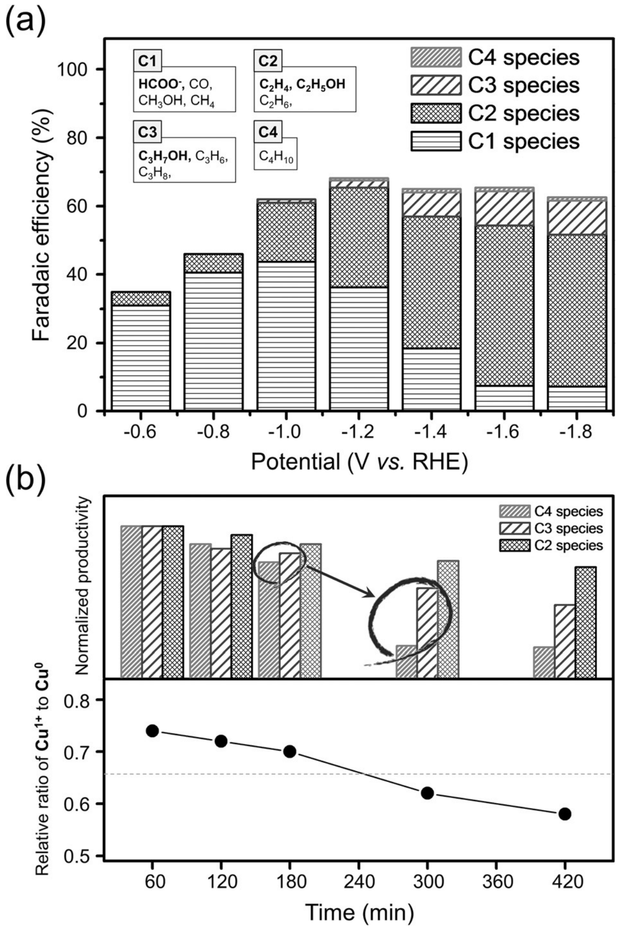

Figure 2. a) Faradaic efficiencies for carbon fuels generated from electrocatalytic conversion of CO_2 on Cu_2O_{Cl} at each cathodic potential. All tests for reaction products analysis were carried out for 1 h. b) Long-term performance over 7 h at −1.6 V (vs. RHE) in 0.1 M KCl (top). Marked circles show the trend of C3–C4 species productivity decreasing more rapidly relative to that for the C2 species as a function of reaction time. Relative ratio of Cu^{1+} to Cu^0 may contribute to the formation of carbon chains (bottom).

Based on the above observations, long-term electrocatalytic conversion was carried out at the selected cathodic potential of −1.6 V (vs. RHE) to investigate the catalytic stability of Cu_2O_{Cl}, considering both the activity and selectivity for production of multi-carbon fuels (Supporting Information, Figure S7). The Cu_2O_{Cl} exhibited a stable productivity toward the C2 species containing mostly C_2H_4 and C_2H_5OH as major products (Figure 2b). In contrast, the productivity for higher carbon number products showed a significant decline compared with that for the C2 products. To understand this observation, bulk and surface-sensitive X-ray spectroscopic techniques were utilized. Using X-ray photoelectron spectroscopy (XPS) analysis, Cu LMM peaks (Supporting Information, Figure S8), with the intense Cu^{1+} peak appearing at 916.5 eV together with a less intense peak corresponding to Cu^0 at 918.45 eV.[15] In particular, formation of the native oxide must be carefully monitored when using such a sensitive surface analyzer. In terms of the exclusion of the native oxide layer, we and others have already demonstrated experimental results in previous studies.[9,16] Recognizing the surface analysis, we compared the ratio of two phases (Cu^{1+} and Cu^0) in surface and bulk regions using XPS and XRD data, respectively, to clarify the state of the electrode. More abundant Cu^{1+} content in surface was confirmed than in bulk region, and Auger depth profiles also described similar oxygen composition (Supporting Information, Table S2, Figures S9, S10).

Based on our previous suggestions,[9] the selectivity in CO_2 catalysis can be affected by the oxidized phase concentration in the surface region, as well as by the oxide-derived metal structure. Owing to the decreasing relative ratio of Cu^{1+} to Cu^0, the lower productivity for C3–C4 species indicates that Cu^{1+} is necessary to provide fuels with carbon chains longer than C3. It is reasonable to conclude that C3–C4 products were not detected on the Cu_2O_{OE} during the CO_2 conversion because of the lower Cu^{1+} to Cu^0 ratio of the catalyst.[9] Apart from the surface activity, previous studies indicate that interstitial residual oxide or oxygen contents at the subsurface should not be underestimated.[16–18]

To exclude local pH factors controlling the product selectivity,[19] we carried out further CO_2 conversion in 0.1 M K_2SO_4 because such KCl and K_2SO_4 are widely known as weak buffer solutions, creating high local pH conditions at the electrode surface.[6] The Cu^{1+} phase was smaller and the trace of n-C_3H_7OH was only observed, although C2 species were rationally produced (Supporting Information, Figure S11). Consequently, the possibility that local pH might affect the formation of C3–C4 species can be excluded. We also studied CO_2 conversion on the Cu metal electrode at −1.6 V (vs. RHE) in 0.1 M KCl. A lower current density was obtained than for Cu_2O_{Cl}, and a different product distribution was observed (Supporting Information, Figure S12). Although C2 species (C_2H_4 and C_2H_5OH) were generated with a Faradaic efficiency of over 20%, higher carbon number products (≥ C3) were not detected. Contrary to other studies, Cl^- was not found to be relevant to CO_2 catalysis,[11] or to serve as a precursor for well-structured metal,[20] but was verified as a delayer on reducing Cu_2O to metallic Cu through investigation of surface composition using XPS and SEM-EDS (Supporting Information, Figures S13, S14). These results clearly support the hypothesis that the distinct catalytic selectivity of Cu_2O_{Cl} towards the C3–C4 species is mainly associated with the oxidized state of Cu_2O_{Cl} itself rather than with the KCl electrolyte or local pH.

To clearly compare the different changes of oxidized states of both Cu_2O_{Cl} and Cu_2O_{OE}, time-dependent changes in the composition of the catalyst were characterized using the in situ X-ray absorption spectroscopy (XAS) apparatus at the Pohang accelerator laboratory (PAL). XANES spectra are strongly sensitive to the chemical state during the CO_2 conversion were observed.[21] As depicted in Figure 3, the pre-edge positions that depend on the Cu oxidation state were shifted toward lower energy values, implying that partial electrochemical reduction of the oxide to the metallic phase occurred during the process time for both electrodes. However, the lower energy shift of pre-edge centroid was smaller for Cu_2O_{Cl} than for Cu_2O_{OE}, and the Cu metal shoulder peak (see dotted circle) at 9003 eV also rapidly appeared for Cu_2O_{OE}.[21] This observation shows that the partial reduction of Cu_2O to Cu was more suppressed in the KCl electrolyte than in $KHCO_3$, and therefore, the higher Cu oxidized phase content on the Cu_2O_{Cl} was confirmed (Supporting Information, Figure S15).

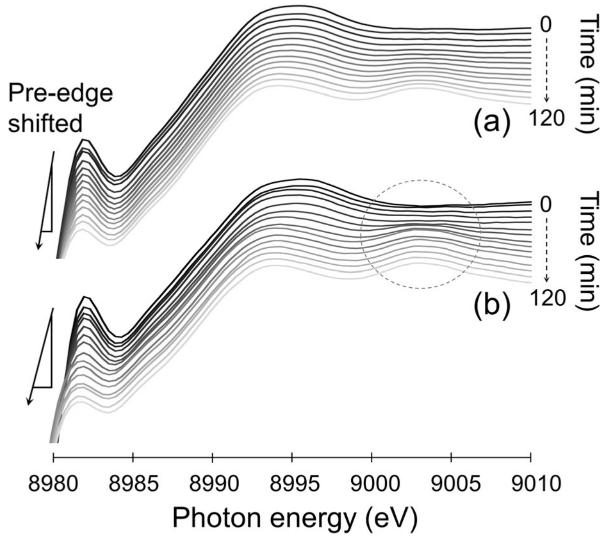

Figure 3. Comparison of in situ measured Cu K-edge XANES results for a) Cu_2O_{Cl} and b) Cu_2O_{OE} as a function of reaction time. In situ experiments were carried out at cathodic potential of −1.6 V (vs. RHE) for 2 h.

Using a variety of analytic techniques such as XRD, XPS, XAS, TEM-EDS, and SEM-EDS, we investigated the Cl-induced bi-phasic Cu_2O catalyst and observed the distinct oxidized phase of the catalyst electrode. The experimental data suggest that the production of the C3–C4 species may be encouraged by the nature of Cu_2O_{Cl}, especially by the higher amount of the residual Cu^{1+} component. In particular, the real-time electrode analysis exhibited C3-C4 compounds generated on a metastable bi-phasic Cu_2O-Cu surface only for a limited reaction time. However, the study of the transient electrocatalysis could help understand a key factor for higher multi-carbon production in CO_2 conversion.

A number of research groups have recently studied the reaction mechanism using density functional theory (DFT) calculations, and several different arguments have been presented for the experimentally unidentified mechanism of CO_2 conversion.[18] Nevertheless, the following series of steps can be considered as a typical underlying mechanism.

$$CO_2\ (g) + {}^* + H^+(aq.) + e^- \rightarrow {}^*HCOO \tag{1}$$

$$CO_2\ (g) + {}^* + H^+\ (aq.) + e^- \rightarrow {}^*COOH \tag{2}$$

$${}^*COOH + H^+\ (aq.) + e^- \rightarrow {}^*CO + H_2O\ (l) \tag{3}$$

$${}^*CO \rightarrow CO\ (g) \tag{4}$$

$${}^*CO + H^+\ (aq.) + e^- \rightarrow {}^*CHO \tag{5}$$

Here, * in all Equations denotes a catalytic active site. In the first step, CO_2 conversion pathways are separated into $HCOO^-$ formation [Eq. (1)] or CO formation [Eqs. (2),(3)].

We only focus on the CO intermediate formation route that presents the possibility for the further conversion to multi-carbon fuels. On metals such as Au and Ag, CO production [Eq. (4)] occurs predominantly due to the weakly bound CO on the surface. However, Cu and Cu-based materials are able to bind CO more strongly for conversion into the various intermediates [Eq. (5)].

The stronger CO adsorption on the Cu^{1+} surface has been studied theoretically[23] and experimentally,[6] and the enhancement of CO adsorption owing to the presence of several ad-atoms such as S, O, and Cl has been reported.[24] Because of the enhanced CO adsorption, various intermediates show a more stable coverage on the catalyst surface and prolong the residence time of the intermediates, thereby presenting greater opportunities for the linkage formation of longer carbon chain species.[25] To prove this hypothesis, CO temperature-programmed desorption (TPD) experiment and voltammetric measurements were conducted.

CO desorption traces measuring CO adsorption strength by TPD are shown in Figure 4a.[26] To clearly identify the desorbed CO signal, the mass-to-charge (m/z) ratio was set at 28. For Cu_2O_{OE}, CO desorption began at 300 K, relatively earlier than for Cu_2O_{Cl}. The observation of a later CO desorption signal for Cu_2O_{Cl} indicates the higher binding energy for CO adsorption with the Cu_2O_{Cl} surface compared to that with the Cu_2O_{OE} surface.[24,26] To evaluate the CO adsorption strength under the actual experimental condition, further voltammograms were obtained at a scan rate of $20\,mV\,s^{-1}$ in N_2 and using CO saturated electrolytes of 0.1 M KCl and 0.1 M $KHCO_3$. The electrochemical experiments proceeded in N_2-saturated conditions at first, and the atmosphere was then replaced with CO (Supporting Information, Figure S16). Finally, N_2 gas was again bubbled into the electrolyte. For both electrolytes, each of the three curves showed the same trends during the procedure. Despite N_2 addition in CO-saturated solution, for Pt-like metals, the voltammograms were generally unchanged, implying that CO remained stable.[6]

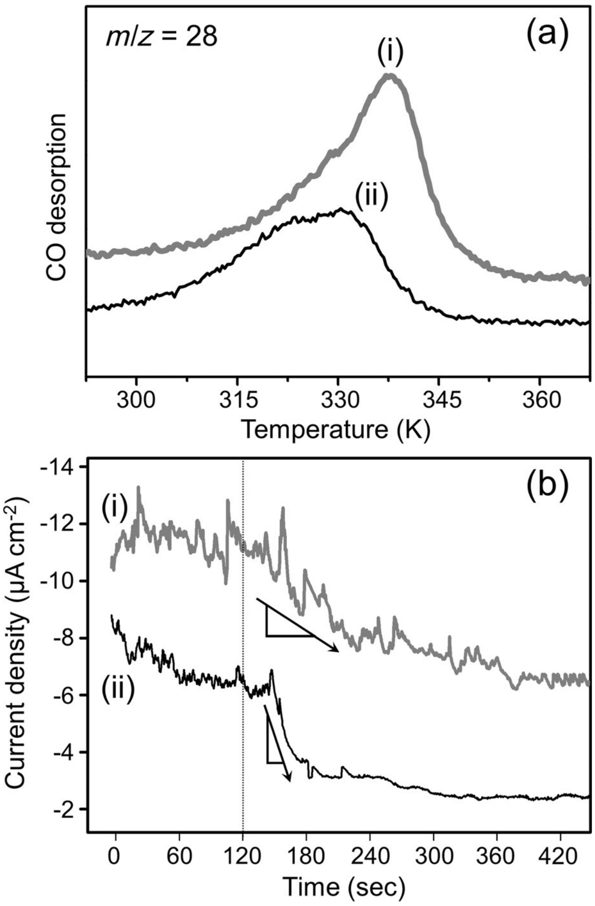

Figure 4. Experimental measurements of CO adsorption strength on the studied catalysts. a) CO TPD profiles of the (i) Cu_2O_{Cl} and (ii) Cu_2O_{OE} at ramping rate of $5\,K\,min^{-1}$. b) Chronoamperometric measurements at constant potential of −0.32 V (vs. RHE; i) in 0.1 M KCl and (ii) 0.1 M $KHCO_3$.

In contrast, for the Cu_2O catalysts, the third curve was in agreement with the first curve, meaning that CO was completely removed by N_2 bubbling. Although we did not observe the different behaviors in cathodic potential sweep between Cu_2O_{Cl} and Cu_2O_{OE}, another measurement (Figure 4b) did show noticeably different results. For CO adsorption on the catalysts in CO-saturated conditions, the electrode potential was kept at −0.32 V (vs. RHE) for 120 s; this potential shows almost a maximum amount of adsorbed CO before the occurrence of any electrochemical reactions. With the addition of N_2 at $30\,mL\,min^{-1}$, the current profiles were measured with the results shown in Figure 4b. Once the N_2 gas was applied after 120 s, the cathodic current decreased more slowly on the Cu_2O_{Cl} than on the Cu_2O_{OE}. Comparison of the slopes of charge variation between the two electrodes shows that Cu_2O_{Cl} exhibits a lower slope, indicating that CO was not easily desorbed compared with Cu_2O_{OE} owing to its relatively higher Cu^{1+}coverage.

In summary, the synergistic effect between the Cu_2O structure and Cl adsorption in an electrocatalytic conversion of CO_2 was studied for the first time. We found that Cu_2O was relatively stabilized and further transformed with the aid of Cl^-. The Cl-induced bi-phasic Cu_2O–Cu was characterized in detail and showed remarkable catalytic ability toward multiple C2–C4 species. In particular, higher carbon number products ($\geq$ C3) were observed with highly significant Faradaic efficiencies of over 10%. Abundance of Cu^{1+} that can strongly bind and preserve the reaction intermediates for a longer time on the surface was demonstrated to be a key factor for the efficient synthesis of longer carbon chain during the CO_2 conversion. At present, although the C3–C4 production is considered as a result of transient reactions and qualitatively dependent on the metastable phase of Cu^{1+}, this result offers a starting point for the development of more suitable catalysts for the CO_2 conversion process into higher multi-carbon products.

Acknowledgements

This study was supported by Basic Science Research Program through the National Research Foundation of Korea (NRF) funded by the Ministry of Education (NRF2013R1A1A2A10063010).

Keywords: bi-phasic Cu_2O–Cu · C3–C4 products · chloride modification · CO adsorption · CO_2 conversion

How to cite: *Angew. Chem. Int. Ed.* **2015**, *54*, 14701 – 14705
Angew. Chem. **2015**, *127*, 14914 – 14918

[1] J. D. Shakun, P. U. Clark, F. He, S. A. Marcott, A. C. Mix, Z. Liu, B. O. Bliesner, A. Schmittner, E. Bard, *Nature* **2012**, *484*, 49 – 54.
[2] J. Qiao, Y. Liu, F. Hong, J. Zhang, *Chem. Soc. Rev.* **2014**, *43*, 631 – 675.
[3] W. Leitner, *Angew. Chem. Int. Ed. Engl.* **1995**, *34*, 2207 – 2221; *Angew. Chem.* **1995**, *107*, 2391 – 2405.
[4] K. Nakata, T. Ozaki, C. Terashima, A. Fujishima, Y. Einaga, *Angew. Chem. Int. Ed.* **2014**, *53*, 871 – 874; *Angew. Chem.* **2014**, *126*, 890 – 893.
[5] J. Lee, Y. Kwon, R. L. Machunda, H. J. Lee, *Chem. Asian J.* **2009**, *4*, 1516 – 1523.
[6] Y. Hori, A. Murata, R. Takahashi, *J. Chem. Soc. Faraday Trans. 1* **1989**, *85*, 2309 – 2326.
[7] C. W. Li, M. W. Kanan, *J. Am. Chem. Soc.* **2012**, *134*, 7231 – 7234.
[8] S. Lee, J. D. Ocon, Y. Son, J. Lee, *J. Phys. Chem. C* **2015**, *119*, 4884 – 4890.
[9] D. Kim, S. Lee, J. D. Ocon, B. Jeong, J. K. Lee, J. Lee, *Phys. Chem. Chem. Phys.* **2015**, *17*, 824 – 830.
[10] a) Y. Bai, T. Yang, Q. Gu, G. Cheng, R. Zheng, *Power Technology* **2012**, *227*, 35 – 42; b) K. Chen, D. Xue, *CrystEngComm* **2013**, *15*, 1739 – 1746; c) M. J. Siegfried, K. S. Choi, *J. Am. Chem. Soc.* **2006**, *128*, 10356 – 10357.
[11] K. Ogura, H. Yano, F. Shirai, *J. Electrochem. Soc.* **2003**, *150*, D163 – D168.
[12] X. L. Deng, S. Hong, I. Hwang, J. S. Kim, J. H. Jeong, Y. C. Park, J. Lee, S. O. Kang, T. Kawai, B. H. Park, *Nanoscale* **2012**, *4*, 2029 – 2033.
[13] K. P. Kuhl, E. R. Cave, D. N. Abram, T. F. Jaramillo, *Energy Environ. Sci.* **2012**, *5*, 7050 – 7059.
[14] G. Centi, S. Perathoner, G. Wine, M. Gangeri, *Green Chem.* **2007**, *9*, 671 – 678.
[15] A. Galtayries, J. P. Bonnelle, *Surf. Interface Anal.* **1995**, *23*, 171 – 179.
[16] Y. Terunuma, A. Saitoh, Y. Momose, *J. Electroanal. Chem.* **1997**, *434*, 69 – 75.
[17] a) H. Bluhm, M. Hävecker, A. Knop-Gericke, E. Kleimenov, R. Schlögl, D. Teschner, V. I. Bukhtiyarov, D. F. Ogletree, M. Salmeron, *J. Phys. Chem. B* **2004**, *108*, 14340 – 14347; b) S. M. Francis, F. M. Leibsle, S. Haq, N. Xiang, M. Bowker, *Surf. Sci.* **1994**, *315*, 282 – 292.
[18] J. Xiao, A. Kuc, T. Frauenheim, T. Heine, *J. Mater. Chem. A* **2014**, *2*, 4885 – 4889.
[19] a) K. J. P. Schouten, E. P. Gallent, M. T. M. Koper, *ACS Catal.* **2013**, *3*, 1292 – 1295; b) R. Kas, R. Kortlever, H. Yilmaz, M. T. M. Koper, G. Mul, *ChemElectroChem* **2015**, *2*, 354 – 358.
[20] a) F. S. Roberts, K. P. Kuhl, A. Nilsson, *Angew. Chem. Int. Ed.* **2015**, *54*, 5179 – 5182; *Angew. Chem.* **2015**, *127*, 5268 – 5271; b) C. S. Chen, A. D. Handoko, J. H. Wan, L. Ma, D. Ren, B. S. Yeo, *Catal. Sci. Technol.* **2015**, *5*, 161 – 168.
[21] H. Liu, F. Zeng, S. Gao, G. Wang, C. Song, F. Pan, *Phys. Chem. Chem. Phys.* **2013**, *15*, 13153 – 13161.
[22] a) A. A. Peterson, F. Abild-Pedersen, F. Studt, J. Rossmeisl, J. K. Norskov, *Energy Environ. Sci.* **2010**, *3*, 1311 – 1315; b) X. Nie, M. R. Esopi, M. J. Janik, A. Asthagiri, *Angew. Chem. Int. Ed.* **2013**, *52*, 2459 – 2462; *Angew. Chem.* **2013**, *125*, 2519 – 2522; c) F. Calle-Vallejo, M. T. M. Koper, *Angew. Chem. Int. Ed.* **2013**, *52*, 7282 – 7285; *Angew. Chem.* **2013**, *125*, 7423 – 7426.
[23] D. F. Cox, K. H. Schulz, *Surf. Sci.* **1991**, *249*, 138 – 148.
[24] L. Y. Gan, Y. J. Zhao, *J. Chem. Phys.* **2010**, *133*, 094703.
[25] a) S. Sen, D. Liu, G. Tayhas, R. Palmore, *ACS Catal.* **2014**, *4*, 3091 – 3095; b) K. G. Schmitt, A. A. Gewirth, *J. Phys. Chem. C* **2014**, *118*, 17567 – 17576.
[26] S. Vollmer, G. Witte, C. Wöll, *Catal. Lett.* **2001**, *77*, 97 – 101.

Received: June 22, 2015
Revised: August 31, 2015